Experiments on a Coupled Oscillator

Feinan N. Yan, S. T. Yip, and H. K. Wong

Abstract—**The theory of a symmetric and asymmetric coupled oscillator circuit with an arbitrary initial condition was verified by a novel experimental technique.**

I. INTRODUCTION

COUPLED oscillators (Fig. 1) are often used in mechanics to explain normal modes [1] and in materials science to model molecule adsorption on crystal surfaces [2]. Each normal mode corresponds to a vibration of the system with only one (resonant) frequency. An arbitrary vibration can be described as a mixed state of these normal modes. An electric oscillator containing capacitors and inductors has analogous essentials, with the inductance, capacitance, voltage, current, and resistance corresponding to the mass, compliance, force, velocity, and friction of a mechanical system, respectively. In addition, an electric coupled oscillator is more nearly ideal than most mechanical oscillators and easy to work with. Some experiments [3] using electric oscillators have been designed to demonstrate normal modes, but they appear to be too simplified. In fact, the circuits used in these experiments are forced and thus not identical to that shown in Fig. 1. The analysis of these forced oscillation circuits is actually quite complicated [4]. To avoid such confusion, we have developed a new method by which the circuit shown in Fig. 1 can be studied theoretically and experimentally without any modification. In this paper, we will explain the method and then use it to study the normal modes and the effect of initial conditions for both symmetric [1], [3] ($C_1 = C_2$) and asymmetric [4] ($C_1 \neq C_2$) coupled oscillators. The experiments are straightforward and easy to follow. The results match the theory very well and thus facilitate the learning of the concept of normal modes as well as the transient characteristics of electric oscillators. The same approach can be extended to nonlinear coupled oscillators that have found many recent applications in neural networks [5] and chaos [6], [7].

II. THEORY

The theory of coupled oscillators for an arbitrary initial condition can be found in some works [8]. To facilitate the interpretation of our experimental results, we found it necessary to outline the theory first. For the coupled oscillator circuit shown in Fig. 1, we may write down the two loop

Manuscript received February 10, 1994; revised June 25, 1996.

The authors are with the Physics Department, The Chinese University of Hong Kong, Shatin, Hong Kong.

Publisher Item Identifier S 0018-9359(96)08741-9.

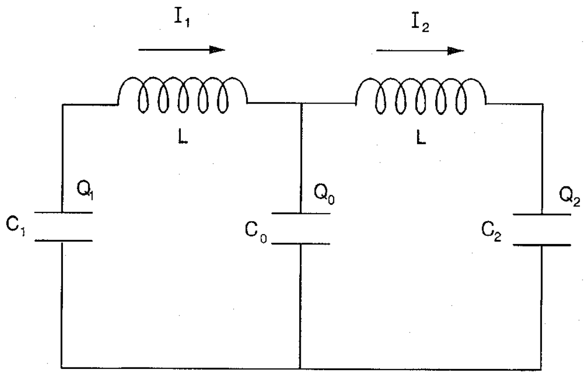

Fig. 1. A coupled oscillator circuit.

equations by Kirchhoff's rules

$$\begin{aligned} \ddot{Q}_1 + \omega_1^2 Q_1 - \lambda Q_0 = 0 \\ \ddot{Q}_2 + \omega_2^2 Q_2 - \lambda Q_0 = 0 \end{aligned} \tag{1}$$

where

$$\omega_1^2 = 1/LC_1, \quad \omega_2^2 = 1/LC_2, \quad \lambda = 1/LC_0. \tag{2}$$

The total charge on the upper part of the circuit is

$$Q = Q_1 + Q_2 + Q_0 \tag{3}$$

which depends on the initial condition of the oscillation and, in general, is a nonzero constant. (Both [3] and [4] assume $Q = 0$.) To simplify (1), we define a voltage V such that

$$Q \equiv (C_1 + C_2 + C_0)V.$$

By also defining

$$q_1 \equiv Q_1 - C_1 V \quad \text{and} \quad q_2 \equiv Q_2 - C_2 V \tag{4}$$

Equation (1) can be rewritten as

$$\begin{aligned} \ddot{q}_1 + \omega_1^2 q_1 + \lambda(q_1 + q_2) = 0 \\ \ddot{q}_2 + \omega_2^2 q_2 + \lambda(q_1 + q_2) = 0. \end{aligned} \tag{5}$$

Equation (5) can be simplified in terms of the normal mode coordinates x_1 and x_2, which are linear combinations of q_1

and q_2

$$\begin{pmatrix} x_1 \\ x_2 \end{pmatrix} = \begin{pmatrix} \cos\phi & \sin\phi \\ -\sin\phi & \cos\phi \end{pmatrix} \begin{pmatrix} q_1 \\ q_2 \end{pmatrix}.$$

By definition, the normal mode coordinates oscillate with frequencies $\omega_\pm$

$$\ddot{x}_1 = -\omega_+^2 x_1$$
$$\ddot{x}_2 = -\omega_-^2 x_2.$$

These require [from (5)]

$$\omega_\pm^2 = \frac{1}{2}\left\{2\lambda + (\omega_1^2 + \omega_2^2) \pm \sqrt{(\omega_1^2 - \omega_2^2)^2 + 4\lambda^2}\right\} \quad (6)$$

and

$$\tan 2\phi = \frac{2\lambda}{\omega_1^2 - \omega_2^2}. \quad (7)$$

We now consider the effect of initial conditions. The capacitors C_1 and C_2 are first charged at dc voltages V_{10} and V_{20}, respectively, i.e., at $t = 0$,

$$Q_1 = C_1 V_{10}$$
$$Q_2 = C_2 V_{20}$$
$$Q_0 = 0$$

and

$$\dot{Q}_1 = \dot{Q}_2 = \dot{Q}_0 = 0.$$

Thus

$$Q = C_1 V_{10} + C_2 V_{20}$$

and

$$V = \frac{C_1 V_{10} + C_2 V_{20}}{C_1 + C_2 + C_0}. \quad (8)$$

The solutions that satisfy this initial condition ($\dot{q}_1 = \dot{q}_2 = 0$) are

$$x_1 = x_{10} \cos \omega_+ t \text{ and } x_2 = x_{20} \cos \omega_- t.$$

The charges on the capacitors are thus given by

$$\begin{aligned} Q_1 &= x_{10} \cos\phi \cos\omega_+ t - x_{20} \sin\phi \cos\omega_- t + C_1 V \\ Q_2 &= x_{10} \sin\phi \cos\omega_+ t + x_{20} \cos\phi \cos\omega_- t + C_2 V \\ Q_0 &= Q - Q_1 - Q_2 \end{aligned} \quad (9)$$

where, as required by the initial condition

$$\begin{aligned} x_{10} &= +C_1(V_{10} - V)\cos\phi + C_2(V_{20} - V)\sin\phi \\ x_{20} &= -C_1(V_{10} - V)\sin\phi + C_2(V_{20} - V)\cos\phi. \end{aligned} \quad (10)$$

For the normal mode with frequency ω_+, $x_{20} = 0$, which requires V_{10} and V_{20} (the initial condition) to satisfy

$$\frac{C_2(V_{20} - V)}{C_1(V_{10} - V)} = \tan\phi \quad (11)$$

where $\tan\phi$ is determined by (7).

Thus, from (9) and (10)

$$\begin{aligned} V_1 &= Q_1/C_1 = (V_{10} - V)\cos\omega_+ t + V \\ V_2 &= Q_2/C_2 = (V_{20} - V)\cos\omega_+ t + V. \end{aligned} \quad (12)$$

Similarly, for the normal mode with frequency ω_-, $x_{10} = 0$ and the initial condition must satisfy

$$\frac{C_1(V_{10} - V)}{C_2(V_{20} - V)} = -\tan\phi. \quad (13)$$

In this mode

$$V_1 = (V_{10} - V)\cos\omega_- t + V$$

and

$$V_2 = (V_{20} - V)\cos\omega_- t + V.$$

For a symmetrically coupled oscillator, $C_1 = C_2$ and $\tan\phi = 1$. From (6), (11), and (13), we get

$$\begin{aligned} \omega_+^2 &= \omega_1^2 + 2\lambda \quad \text{when } V_{20} = V_{10}, \\ \omega_- &= \omega_1 \quad \text{when } V_{20} = -V_{10}. \end{aligned} \quad (14)$$

The expression for ω_+ clearly indicates that the coupling strength is stronger for smaller C.

In practice, the circuit unavoidably carries a nonzero resistance R in each loop. All previous equations for Q_1, Q_2, V_1, and V_2 must be modified by the insertion of a damping factor $e^{-Rt/2L}$; e.g., (12) should be rewritten as

$$\begin{aligned} V_1 &= (V_{10} - V)e^{-Rt/2L}\cos\omega_+ t + V \\ V_2 &= (V_{20} - V)e^{-Rt/2L}\cos\omega_+ t + V. \end{aligned} \quad (15)$$

III. Experiment

The circuit used in our experiments is illustrated in Fig. 2(a). For clarity we highlighted the coupled oscillator configuration as that shown in Fig. 1. With the help of five switches, we can set up any initial condition required for a particular oscillation. These switches are controlled by a square wave generator (operated at a frequency of 1–3 kHz). Their positions are listed in Fig. 2(b). State 1 is for setting up the initial conditions. In state 2, the circuit becomes exactly the same as shown in Fig. 1. In other words, the same circuit is used in both the theoretical analysis and the experimental study. This will eliminate the confusion that can arise in previous approaches. In order to reduce the damping of the oscillations, S_4 and S_5 must have very small contact resistances. Initial efforts using relay switches were not successful because of their slow speed, high contact resistance, and bouncing contact problems. The integrated-circuit industry has developed a number of solid-state switches for high-speed operations, and these so-called analog switches have become commercially available. We have tested many analog switches and found that only

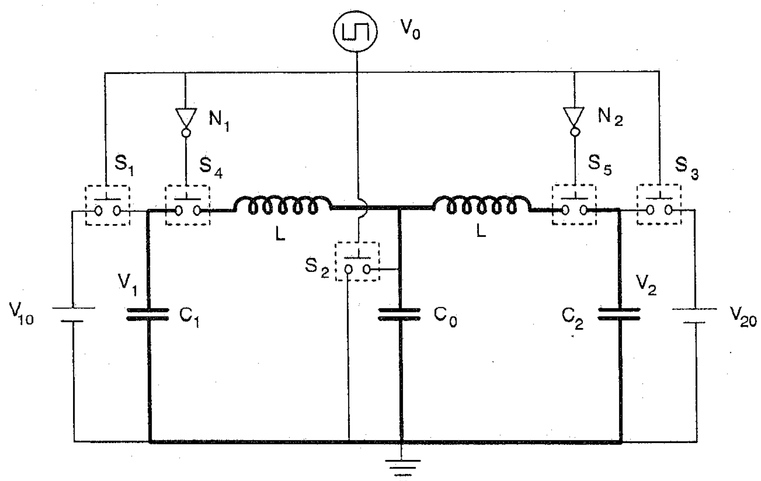

(a)

state	sig. gen.	switch				
	V_0	S_1	S_2	S_3	S_4	S_5
1	low	on	on	on	off	off
2	high	off	off	off	on	on

(b)

Fig. 2. (a) Schematic diagram of the circuit for the experiments. The square wave generator was operated at 1–3 kHz. We used DG180BA for switches S_1, S_3, S_4, and S_5; DG411DJ for S_2; and 7400S1 for the inverters. (b) Positions of switches.

DG180BA [9], which has less than 10 Ω resistance when closed, can fulfill the requirements. Identical inductors with $L = 860 \pm 2$ μH and dc resistance less than 1.2 Ω were selected for these experiments. The values of L and C were measured with a universal bridge. The voltages across C_1 and C_2 were measured with a low-cost digital storage oscilloscope that was interfaced to a PC for data storage and analysis. The oscillation data V_1 and V_2 were fitted to the derived equations using a commercial software package called PEAK-FIT [10].

IV. Results

A. Symmetric Coupled Oscillator

Normal Modes: Identical capacitors with $C_1 = C_2 = C_0 = 39.2 \pm 0.2$ nF were selected for this experiment. Fig. 3 shows some typical results. Fig. 3(a) and (b) illustrates the two pure normal mode oscillations. Fig. 3(c) is a typical graph for other initial conditions. These data can be fitted with (15) and the fitting parameters give us the normal mode frequencies ($f_\pm = \omega_\pm/2\pi$), the damping time constant ($2L/R$), and the value of V as given by (8).

Coupling Strength: In this experiment, we measured $\omega_\pm$ as a function of C_0. The result is shown in Fig. 4. The lines on the graph were drawn according to (14).

Energy Transfer: In this experiment we set $V_{10} = 5$ V and $V_{20} = 0$. For this initial condition

$$V_1 = (V_{10} - V)e^{-Rt/2L} \cos\left(\frac{\omega_+ + \omega_-}{2}t\right) \cos\left(\frac{\omega_+ - \omega_-}{2}t\right) + V$$
$$V_2 = (V_{10} - V)e^{-Rt/2L} \sin\left(\frac{\omega_+ + \omega_-}{2}t\right) \sin\left(\frac{\omega_+ - \omega_-}{2}t\right) + V.$$

Fig. 5 shows the oscillations of V_1 and V_2 demonstrating the energy transfer phenomena. The effect is more conspicuous for large values of C_0. The time required for energy to transfer back and forth is

$$t_0 = \frac{2\pi}{\omega_+ - \omega_-}. \quad (16)$$

We measured t_0 as a function of C_0 and the result is plotted in Fig. 6. The curve on the graph was drawn according to (16).

B. Asymmetric Coupled Oscillator

Normal Modes: As we discussed in the theory section, the initial conditions required to observe normal modes in an asymmetric coupled oscillator [expressed by (11) and (13)] are not as simple as in a symmetric coupled oscillator [(14)].

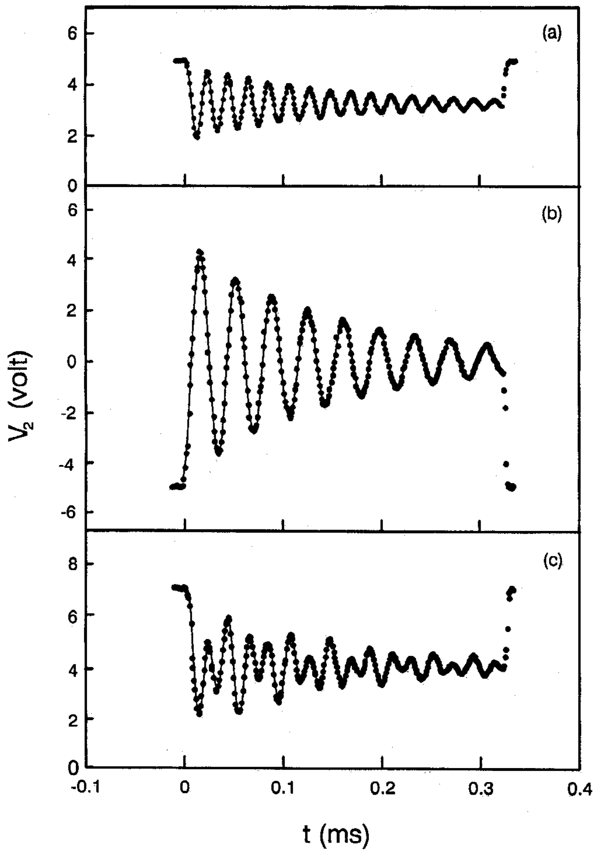

Fig. 3. Oscillation graphs for the symmetric coupled oscillator. The curves are simulations with fitting parameters $f_- = 27.4$ kHz, $f_+ = 47.5$ kHz, and $R = 11.4\ \Omega$: (a) $V_{10} = V_{20} = 5$ V. (b)$V_{10} = -V_{20} = 5$ V, (c) $V_{10} = 5$ V, $V_{20} = 7$ V.

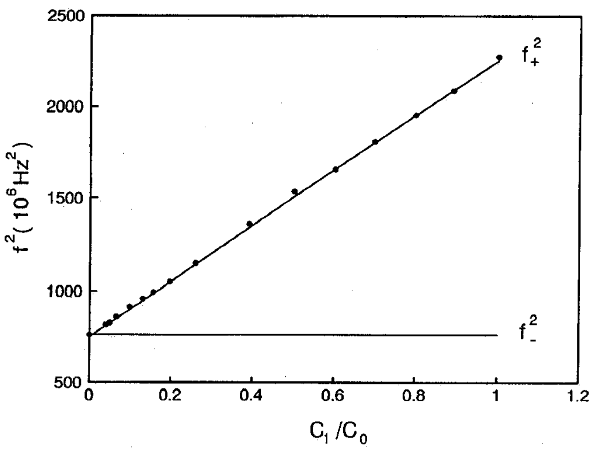

Fig. 4. Normal mode frequencies for the symmetric coupled oscillator. The lines were drawn according to (14).

For each combination of C_1 and C_2, we need to adjust the initial conditions (e.g., vary V_{10} with V_{20} fixed) to achieve $\omega_\pm$ normal mode oscillations [i.e., exhibiting behavior like that

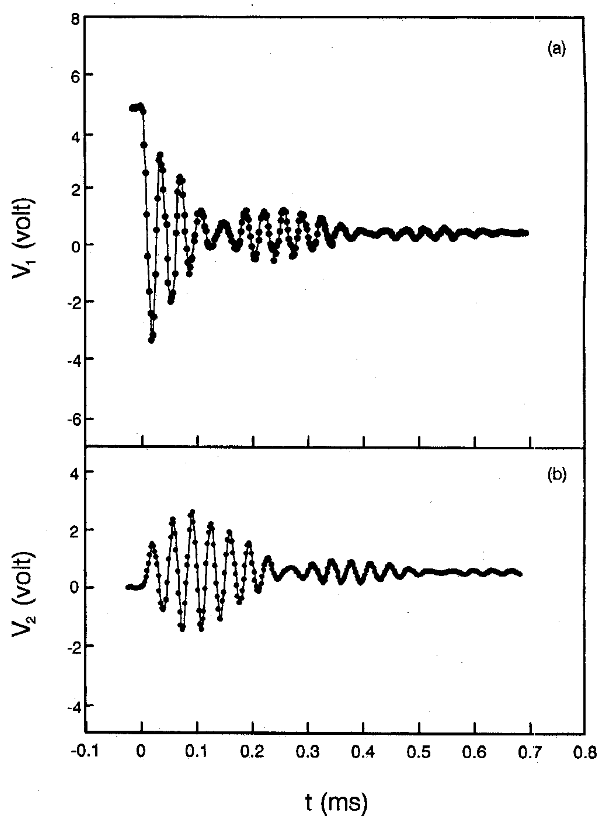

Fig. 5. Demonstration of energy transfer. Initial condition here was $V_{10} = 5$ V, $V_{20} = 0$.

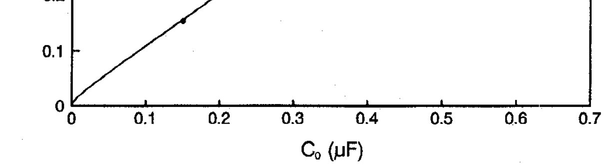

Fig. 6. Time of energy transfer t_0 as a function of C_0. The curve was drawn according to (16).

in Fig. 3(a) and (b)]. The results for various combinations of C_1 and C_2 are plotted in Fig. 7, which shows that the initial conditions for normal mode oscillations can be predicted very well by (11) and (13).

Normal Mode Frequencies: The normal mode frequencies are given in (6). To verify these complicated expressions, we

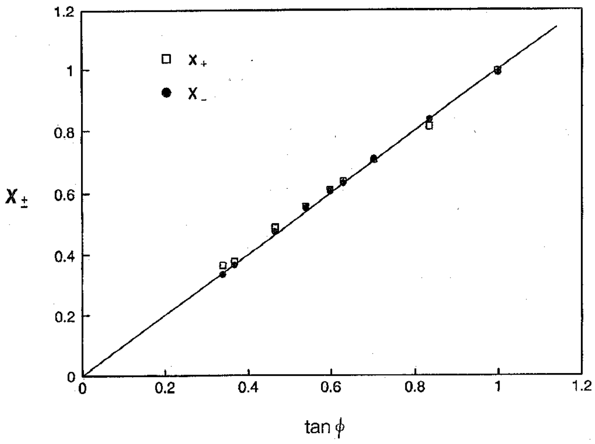

Fig. 7. The initial conditions of normal mode oscillations for various combinations of C_1 and C_2, where $X_+ \equiv \frac{C_2(V_{20}-V)}{C_1(V_{10}-V)}$, $X_- \equiv -\frac{C_1(V_{10}-V)}{C_2(V_{20}-V)}$, and tan ϕ was calculated using (7). The line shown was drawn according to (11) and (13).

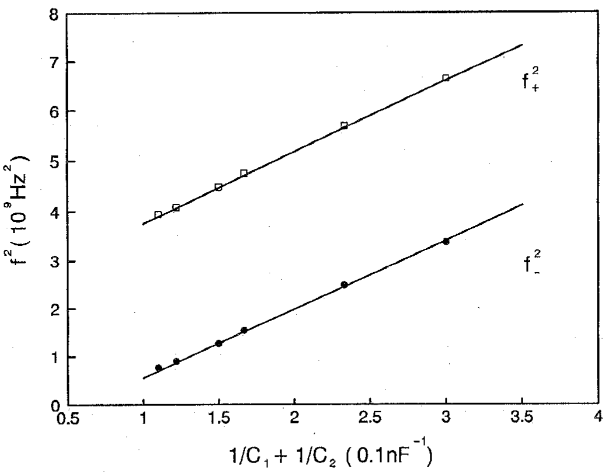

Fig. 8. Normal mode frequencies as a function of $\frac{1}{C_1} + \frac{1}{C_2}$ with $\frac{1}{C_1} - \frac{1}{C_2} = \frac{1}{10}(\text{nF})^{-1}$. The lines were drawn according to (6).

varied C_1 and C_2 such that $\frac{1}{C_1} - \frac{1}{C_2} = \frac{1}{10}$ $(\text{nF})^{-1}$ (i.e., $\omega_1^2 - \omega_2^2$ was kept constant). Following the procedures described in Section IV-B, we obtained the values of $\omega_\pm$ and plotted them as a function of $\frac{1}{C_1} + \frac{1}{C_2}$ (see Fig. 8). The straight lines in the plot were drawn according to (6).

V. Conclusion

We have presented the theory for a symmetric and asymmetric coupled oscillator with arbitrary initial conditions. All theoretical results were verified by experiments. The key for the success of these experiments is the use of the analog switches. These new electronic devices are very fast and have very low contact resistance when closed. With the help of these novel switches, one can set up any initial condition and place the circuit in a configuration identical to the one studied in theory, allowing direct comparison between theory and experiment. This new approach can be easily extended to other more complicated circuits, such as anharmonic coupled oscillators [6], [7], coupled oscillating neural networks [5], and lumped LC transmission lines [11], etc. The technique is especially useful in studying the transient states of an electrical system and chaos in a nonlinear coupled oscillator, both of which depend on the initial conditions [6], [7].

Acknowledgment

The authors appreciate the helpful discussions with C. F. Lo and the technical assistance of W. K. Chao. They also thank C. C. Cheung and H. K. Won for their preliminary experiments.

References

[1] F. S. Crawford, Jr., *Waves*. New York: McGraw-Hill, 1968, pp. 27–28.

[2] F. M. Hoffmann, "Infrared reflection-absorption spectroscopy of absorbed molecules," *Surf. Sci. Rep.*, vol. 3, pp. 107–192, 1983.

[3] A. M. Portis, *Laboratory Physics*. New York: McGraw-Hill, pt. B, 1965, pp. 39–45.

[4] N. W. McLachlan, *Theory of Vibration*. New York: Dover, 1951, pp. 62–64.

[5] J. G. Taylor and C. L. T. Mannion, Eds., *Coupled Oscillating Neurons*. London: Springer-Verlag, 1992.

[6] C. Hayashi, *Nonlinear Oscillations in Physical Systems*. Princeton, NJ: Princeton University Press, Part III, 1985.

[7] T. Yamada, K. Fukushima, and T. Yazaki, *Phase Transitions*, vol. 29, pp. 15–20, 1990.

[8] K. R. Symon, *Mechanics*, 3rd ed. Reading, MA: Addison-Wesley, 1971, pp. 191–197.

[9] DG180BA and DG411DJ are supplied by Siliconix Inc., 2201 G Laurelwood Rd., Santa Clara, CA 95054 USA.

[10] Product of Jandel Scientific, 2591 Kerner Blvd., San Rafael, CA 94901, USA.

[11] R. C. Cross, *Amer. J. Phys.*, vol. 53, pp. 563–567, 1985.

Feinan N. Yan received the B.Sc. and M.Sc. degrees in physics from the University of Science & Technology, ROC, in 1984 and 1987, respectively.

She is a Teacher in the Fundamental Physics Center, University of Science & Technology. In 1993 she visited the Chinese University of Hong Kong, Hong Kong and performed the experiments presented in this paper.

S. T. Yip received the B.Sc. and M.Ph. degrees in physics from the Chinese University of Hong Kong, Hong Kong, in 1982 and 1984, respectively.

He became the Technician at the Chinese University of Hong Kong, and is now the Laboratory Safety Officer and Radiation Protection Officer.

H. K. Wong received the Ph.D. degree in physics from Northwestern University, Evanston, IL, in 1985.

After a period as a Visiting Scientist at the IBM Research Laboratory, San Jose, CA, he joined the Physics Department of the Chinese University of Hong Kong, Hong Kong. He is currently Associate Professor. His research concentrates on thin film physics.